Electr Eng (2011) 93:33–42
DOI 10.1007/s00202-010-0187-x

ORIGINAL PAPER

Effects of STATCOM, TCSC, SSSC and UPFC on static voltage stability

Mehrdad Ahmadi Kamarposhti · Hamid Lesani

Received: 28 July 2009 / Accepted: 6 November 2010 / Published online: 3 December 2010

Abstract The purpose of this paper is to study the effects of four FACTS controllers: STATCOM, TCSC, SSSC and UPFC on static voltage stability in power systems. Continuation power flow is used to evaluate the effects of these devices on system loadability. Applying saddle node bifurcation theory with the use of PSAT, effects of these devices controllers on maximum loading point are determined. Static voltage stability margin enhancement using STATCOM, TCSC, SSSC and UPFC is compared in the modified IEEE 14-bus test system.

Keywords Voltage collapse · Static voltage stability · STATCOM · TCSC · SSSC · UPFC

Abbreviations

CPF	Continuation power flow
MLP	Maximum loading point
FACTS	Flexible AC transmission system
SVC	Static var compensator
STATCOM	Static synchronous compensator
TCSC	Thyristor-controlled series capacitor
SSSC	Static synchronous series compensator
UPFC	Unified power flow controller
MWM	Mega Watt margin
VSI	Voltage-source inverter
TCR	Thyristor-controlled reactor
GTOs	Gate turn-off thyristors
PSAT	Power system analysis toolbox
λ_{max}	Maximum load parameter
P_{max}	Maximum load active power corresponding with MLP
P_{base}	Base load active power

M. A. Kamarposhti (✉)
Department of Electrical Engineering, Islamic Azad University, Jouybar Branch, Jouybar, Iran
e-mail: M.Ahmadi@jouybariau.ac.ir

H. Lesani
Department of Electrical Engineering, University of Tehran, Tehran, Iran
e-mail: lesani@ut.ac.ir

1 Introduction

Voltage instability is mainly associated with reactive power imbalance. The loadability of a bus in the power system depends on the reactive power support that the bus can receive from the system as the system approaches the maximum loading point (MLP) or voltage collapse point, both real and reactive power losses increase rapidly. Therefore, the reactive power supports have to be local and adequate.

There are two types of voltage stability based on the time frame of simulation: static voltage stability and dynamic voltage stability. Static analysis involves only the solution of algebraic equations and therefore is computationally less extensive than dynamic analysis. Static voltage stability is ideal for the bulk of studies in which voltage stability limit for many pre-contingency and post-contingency cases must be determined.

In static voltage stability, slowly developing changes in the power system occur that eventually lead to a shortage of reactive power and declining voltage. This phenomenon can be seen from the plot of the power transferred versus the voltage at receiving end. The plots are popularly referred to as P–V curve or "Nose" curve. As the power transfer

increases, the voltage at the receiving end decreases. Eventually, the critical (nose) point, the point at which the system reactive power is short in supply, is reached where any further increase in active power transfer will lead to very rapid decrease in voltage magnitude. Before reaching the critical point, the large voltage drop due to heavy reactive power losses can be observed.

The only way to save the system from voltage collapse is to reduce the reactive power load or add additional reactive power prior to reaching the point of voltage collapse [1].

Voltage collapse phenomena in power systems have become one of the important concerns in the power industry over the last two decades, as this has been the major reason for several major blackouts that have occurred throughout the world including the recent Northeast Power outage in North America in August 2003 [2]. Point of collapse method and continuation method are used for voltage collapse studies [3]. Of these two techniques, continuation power flow (CPF) method is used for voltage analysis. These techniques involve the identification of the system equilibrium points or voltage collapse points where the related power flow Jacobian becomes singular [4,5].

Usually, placing adequate reactive power support at the "weakest bus" enhances static voltage stability margins. The weakest bus is defined as the bus, which is nearest to experiencing a voltage collapse. Equivalently, the weakest bus is one that has a large ratio of differential change in voltage to differential change in load ($\partial V/\partial P_{\text{total}}$). Changes in voltage at each bus for a given change in system load are available from the tangent vector, which can be readily obtained from the predictor steps in the CPF process. In addition to the above method, the weakest bus could be obtained by looking at right eigenvectors associated with the smallest eigenvalue as well.

Reactive power support can be done with FACTS devices. Each FACTS device has different characteristics; some of them may be problematic as far as the static voltage stability is concerned. Therefore, it is important to study their behaviors in order to use them effectively.

Canizares and Faur [6] studied the effects of SVC and TCSC on voltage collapse. In [7], voltage stability assessment of the system with shunt compensation devices including shunt capacitors, SVC and STATCOM is studied and compared in the IEEE 14-bus test system. Study of STATCOM and UPFC controllers for voltage stability evaluated by Saddle-Node bifurcation analysis is carried out in [8].

So far, no work has been reported in open literature for the effects of STATCOM, TCSC, SSSC and UPFC on voltage stability. This paper considers four FACTS controllers in order to increase the loadability margin. The aim of this paper is to compare some FACTS devices, namely, STATCOM, TCSC, SSSC and UPFC, in terms of MLP and so its corresponding MWM in static voltage stability study.

Rest of the paper is organized as follows: The mathematical tools needed for voltage collapse studies are discussed in Sect. 2. A brief introduction of the stability models including DC representations of STATCOM, TCSC, SSSC and UPFC is presented in Sect. 3. Section 4 examines the effects of these controllers on voltage collapse using a 14-bus test system. Section 5 reviews the main points discussed in this paper.

2 Power systems as differential algebraic dynamical systems

Mathematical models of power systems generally consist of a set of parameter-dependent differential and algebraic equations in the form [9,10]:

$$\dot{x} = f(x, y, p), \quad f : R^{n+m+q} \to R^n \tag{1}$$

$$0 = g(x, y, p), \quad g : R^{n+m+q} \to R^m \tag{2}$$

$$x \in X \subset R^n, \quad y \in Y \subset R^m, \quad p \in P \subset R^q$$

In the state space $X \times Y$, dynamic state variables x such as the dynamic states of generators, loads, etc. and instantaneous variables y corresponding to the steady state element models are distinguished. The dynamics of the states x is defined by Eq. (1), and the dynamics of the y variables is such that system satisfies the constraints (Eq. 2); the parameter p defines a specific system configuration and the operation condition. The system model can be reduced by the term:

$$\dot{x} = f(x, h(x, p), p) = s(x, p) \tag{3}$$

A saddle node bifurcation of the system (3) occurs when the Jacobian $D_x s(x, p)$ is singular at equilibrium point (z_0, p_0), where two solutions of the system, stable and unstable, merge and then disappear as the parameter p, i.e. system load changes. In other words, the Saddle-Node bifurcation point is the voltage collapse point of the system where determinant of the Jacobian will be zero. At least one of the eigenvalues of the Jacobian matrix will become zero, one eigenvalue will change the sign, and system will lose its dynamic voltage stability [11–13].

From the eigenvectors at the bifurcation point, we can provide information on the area prone to voltage collapse point and the control strategies to most effectively prevent this problem.

Theoretically, Saddle-Node bifurcation can occur between a stable equilibrium point and an unstable equilibrium point which can be depicted by Fig. 1. Two known basic tools based on bifurcation theory are direct and continuation methods and are used to compute the voltage collapse point. There are four types of FACTS devices considered in this study, namely, STATCOM, TCSC, SSSC and UPFC. Details including basic

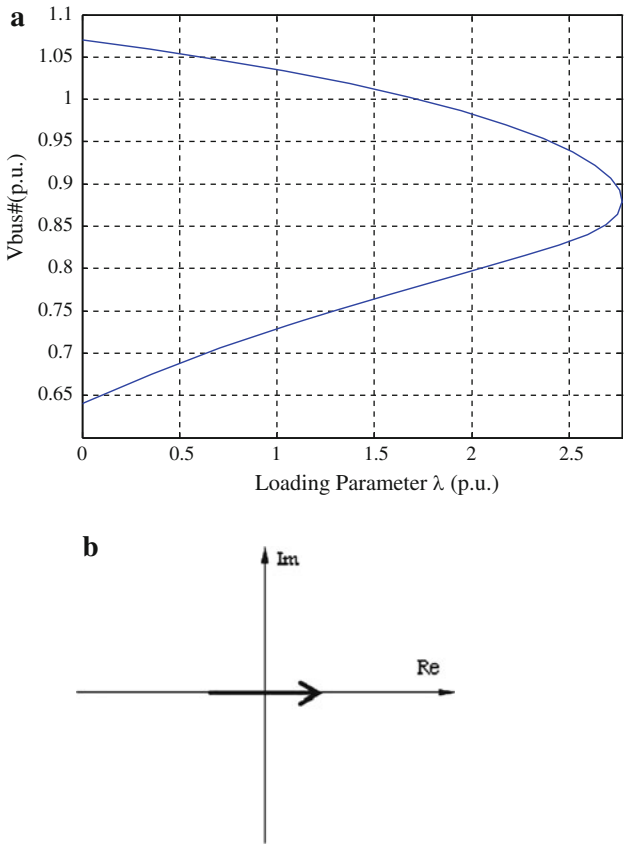

Fig. 1 Saddle-Node bifurcation: **a** bifurcation curve and **b** eigenvalue trajectory

structures and terminal characteristics of these FACTS devices are presented in the following section.

3 STATCOM, TCSC, SSSC and UPFC

It is well-known fact that FACTS devices can be used to provide reactive power compensation. Although there are many types of the FACTS devices, each of them has it own characteristics [14]. Thus, it would be useful to know what type among STATCOM, TCSC and SSSC could give the most benefit in terms of voltage stability margin. Description and terminal characteristics of these FACTS devices are given in the next subsections. Each model is described by a set of differential algebraic equations [8]:

$$\begin{aligned} \dot{x_c} &= f_c\,(x_c, x_s, V, \theta, u) \\ \dot{x_s} &= f_s\,(x_c, x_s, V, \theta) \\ P &= g_p\,(x_c, x_s, V, \theta) \\ Q &= g_p\,(x_c, x_s, V, \theta) \end{aligned} \tag{4}$$

where x_c are the control system variables, x_s are the controlled state variables (e.g. firing angles), and the algebraic variables V and θ are the voltage amplitudes and phases at the buses at which the components are connected, they are vectors in case of series components. Finally, the variable u represents the input control parameters, such as reference voltages or reference power owns.

3.1 STATCOM

STATCOM is the VSI, which converts a DC input voltage into AC output voltage in order to compensate the active and reactive power needed by the system [15,16].

Figures 2 and 3 show the schematic diagram and terminal characteristic of STATCOM, respectively. From Fig. 2, STATCOM is a shunt-connected device, which controls the voltage at the connected bus to the reference value by adjusting voltage and angle of internal voltage source. From Fig. 3, STATCOM exhibits constant current characteristics when the voltage is low/high under/over the limit. This allows STATCOM to deliver constant reactive power at the limits compared to SVC.

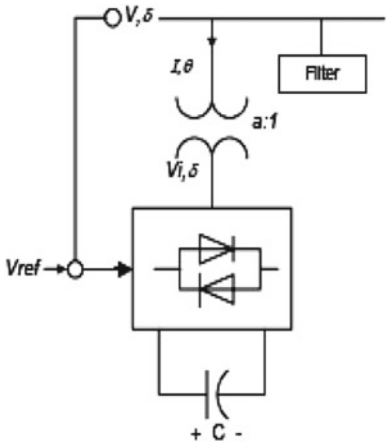

Fig. 2 Basic structure of STATCOM

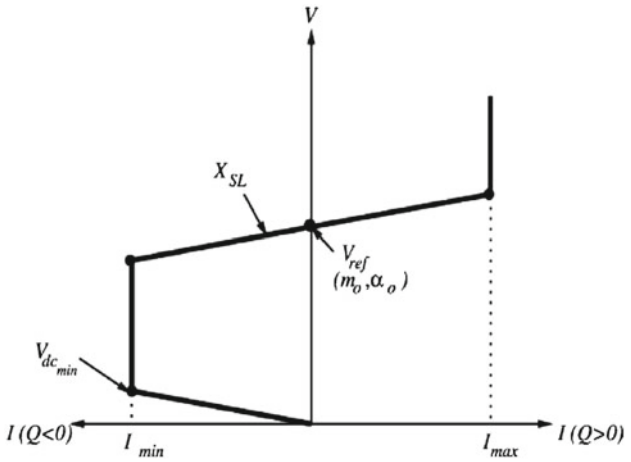

Fig. 3 Terminal characteristic of STATCOM

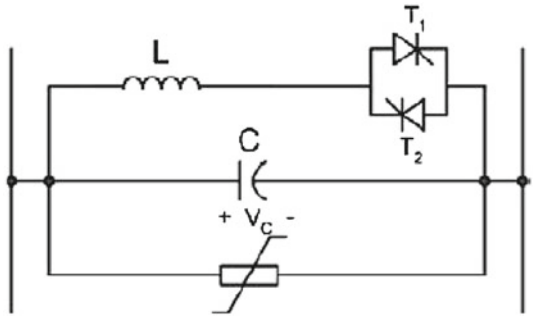

Fig. 4 The basic structure of TCSC

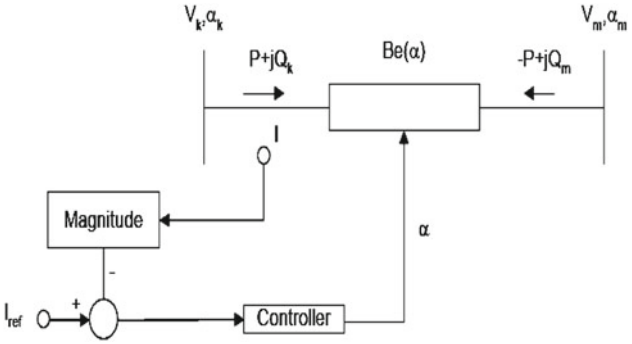

Fig. 5 Stability model of TCSC

3.2 TCSC

TCSC device uses TCR in parallel with capacitor segments of series capacitor bank. The basic structure and stability model of the device are shown in Figs. 4 and 5, respectively [16]. From Figs. 4 and 5, the combination of TCR and capacitor allows the capacitive reactance to be smoothly controlled over a wide range. The value of susceptance (B_e) of the line can be controlled according to a specific controlled variable.

The characteristic of the TCSC depends on the relative reactance of the capacitor bank and thyristor branch. The resonance frequency (ω_r) of LC is expressing as [17]:

$$X_C = -\frac{1}{\omega_n C} \tag{5}$$

$$X_L = \omega L \tag{6}$$

$$\omega_r = \frac{1}{LC} = \omega_n \sqrt{\frac{-X_C}{X_L}} \tag{7}$$

The principle of TCSC in voltage stability enhancement is to control the transmission line impedance by adjusting the TCSC impedance. The absolute impedance of TCSC, which can be adjusted in three modes:

- Blocking mode: The thyristor is not triggered and TCSC is operating in pure capacity in which the power factor of TCSC is leading.

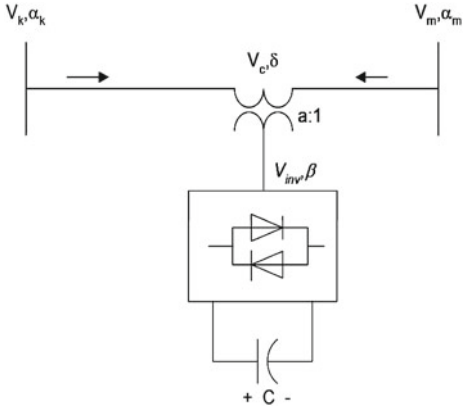

Fig. 6 Basic structure of SSSC

- By pass mode: The thyristor is operated in order to $X_L = X_C$. The current is in phase with TCSC voltage.
- Capacitive boost mode: $X_C > X_L$ and then inductive mode $X_L > X_C$.

3.3 SSSC

SSSC is a solid-state synchronous voltage source employing an appropriate DC to AC inverter with gate turn-off thyristor (GTO). It is similar to the STATCOM, as it is based on a DC capacitor fed VSI that generates a three-phase voltage, which is then injected in a transmission line through a transformer connected in series with the system.

The main control objective of the SSSC is to directly control the current, and indirectly the power, flowing through the line by controlling the reactive power exchange between the SSSC and the AC system. The main advantage of this controller over a TCSC is that it does not significantly affect the impedance of the transmission system and, therefore, there is no danger of having resonance problem [1].

Figures 6 and 7 show basic structure and the representing model of SSSC with control and state variables, respectively. From Figs. 6 and 7, it can be seen that SSSC can absorb/deliver both active and reactive power by controlling voltage and angle at the DC voltage. However, the amount of active power is normally small since the value of RC is small.

3.4 UPFC

The basic components of the UPFC are two VSI using GTO sharing a common DC storage capacitor, and connected to the system through coupling transformers (Fig. 8).

VSI is connected in shunt to the transmission system via a shunt transformer, while the other one is connected in series through a series transformer. The shunt inverter is operating in such a way to inject a controllable current Iq into the

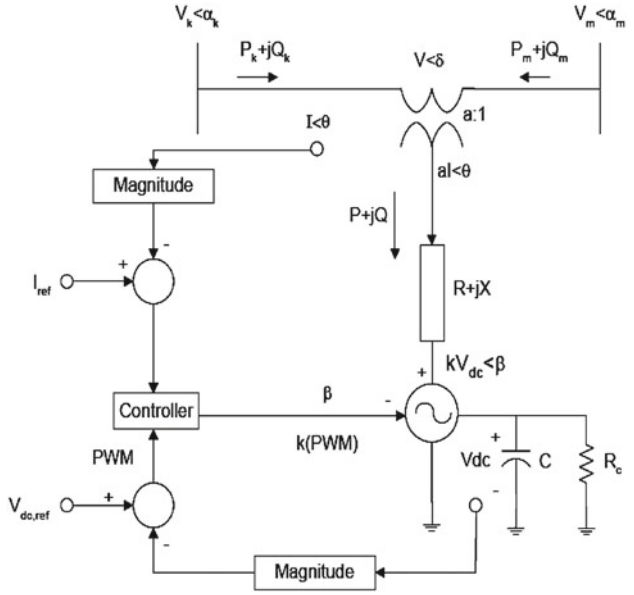

Fig. 7 Stability model of SSSC

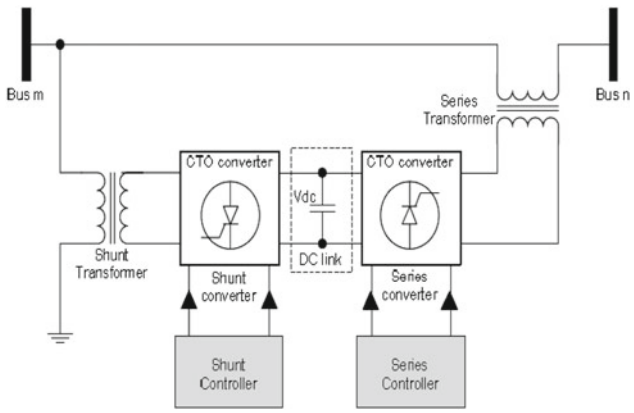

Fig. 8 Basic scheme of a UPFC

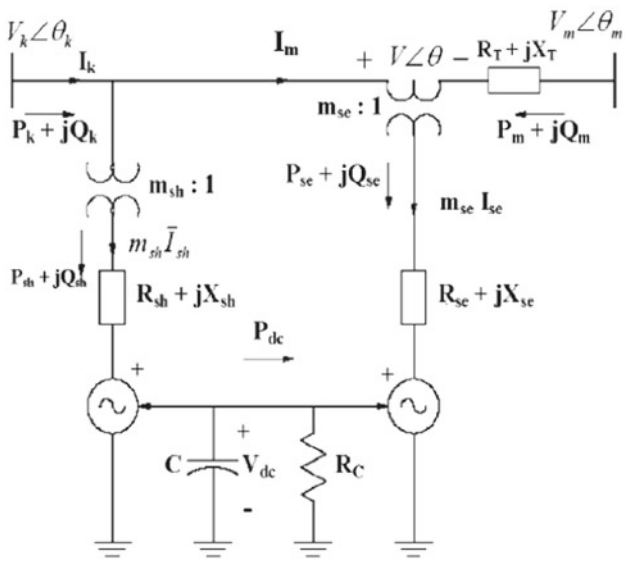

Fig. 9 Stability model of UPFC

transmission line. This current consists of two components with respect to the line voltage. These components are the real or direct component, which is in phase or in possible phase with the line voltage, and the reactive or quadrature component, which is in quadrature [18].

The UPFC model is shown in Fig. 9. According to this figure, there are some parameters that can be adjusted for keeping voltage level and power flow of the network.

4 Voltage stability study with FACTS devices using CPF

Changes in voltage at each bus for a given change in system load are available from the tangent vector, which can be readily obtained from the predictor steps in CPF process. Using reformulated power flow equations, the differential change in the system active power is:

$$\mathrm{d}P_{\text{total}} = C\,\mathrm{d}\lambda \tag{8}$$

Thus, the weakest bus would be:

$$\text{BUS} = \max\left\{\left|\frac{\mathrm{d}V_1}{C\,\mathrm{d}\lambda}\right|, \left|\frac{\mathrm{d}V_2}{C\,\mathrm{d}\lambda}\right|, \ldots, \left|\frac{\mathrm{d}V_n}{C\,\mathrm{d}\lambda}\right|\right\} \tag{9}$$

Since the value of $C\,\mathrm{d}\lambda$ is the same for each $\mathrm{d}V$ elements in given tangent vector, choosing the weakest bus is as easy as choosing the bus with largest $\mathrm{d}V$ component. In addition to the above method, weakest bus could be obtained by looking at the right eigenvectors associated with the smallest eigenvalue as well.

Usually, placing adequate reactive power support at the weakest bus enhances static voltage stability margins. To incorporate FACTS devices in the power system, equations and state variables of FACTS devices are introduced in the load flow equations and in the corrector step in the CPF process. The way to solve the new load flow equations is similar to that in conventional load flow equations but with equations of FACTS devices. Each FACTS device has its own equations and state variables [1].

The number of state variables is as same as the number of FACTS equations required in the load flow formulation. Flowchart of voltage stability with FACTS using the CPF method is illustrated in Fig. 10. From Fig. 10, it can be observed that equations of FACTS devices are added in the load flow equations.

The new load flow equations are then used in the corrector step in CPF process. In the following section, the IEEE 14-bus test system and analysis tools used in the paper are presented in brief and static voltage stability margin enhancement using STATCOM, TCSC, SSSC and UPFC is compared in the modified IEEE 14-bus test system.

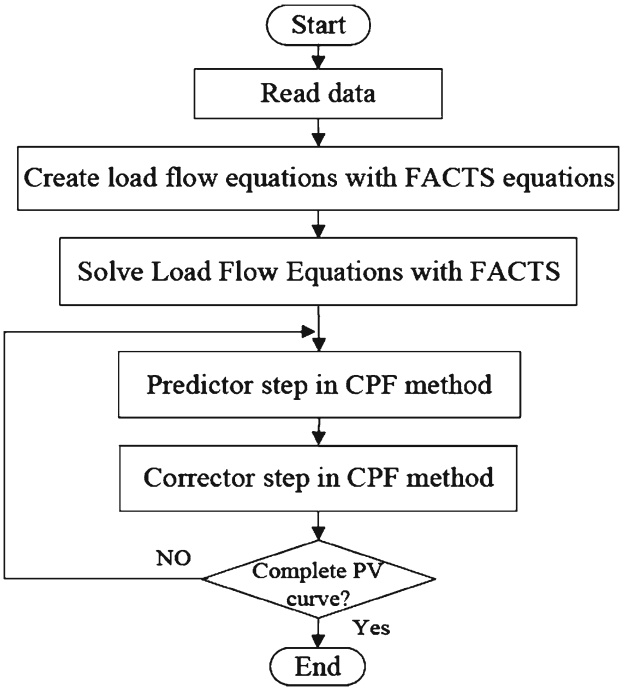

Fig. 10 Flowchart of CPF process with FACTS

5 Simulation results

IEEE 14-bus test system as shown in Fig. 11 is used for voltage stability studies. The test system consists of 5 generators and 11 PQ bus (or load bus). The simulations use PSAT simulation software [19]. PSAT is power system analysis software, which has many features including power flow and CPF. Using CPF feature of PSAT, voltage stability of the test system is investigated.

The behavior of the test system with and without FACTS devices under different loading conditions is studied. The location of the FACTS controllers is determined through bifurcation analysis. A typical PQ model is used for the loads and the generator limits are ignored. Voltage stability analysis is performed by starting from an initial stable operating point and then increasing the loads by a factor λ until singular point of power flow linearization is reached. The loads are defined as:

$$P_{\mathrm{L}} = P_{\mathrm{L0}}\,(1+\lambda)$$
$$Q_{\mathrm{L}} = Q_{\mathrm{L0}}\,(1+\lambda) \tag{10}$$

Fig. 11 The IEEE 14-bus test system

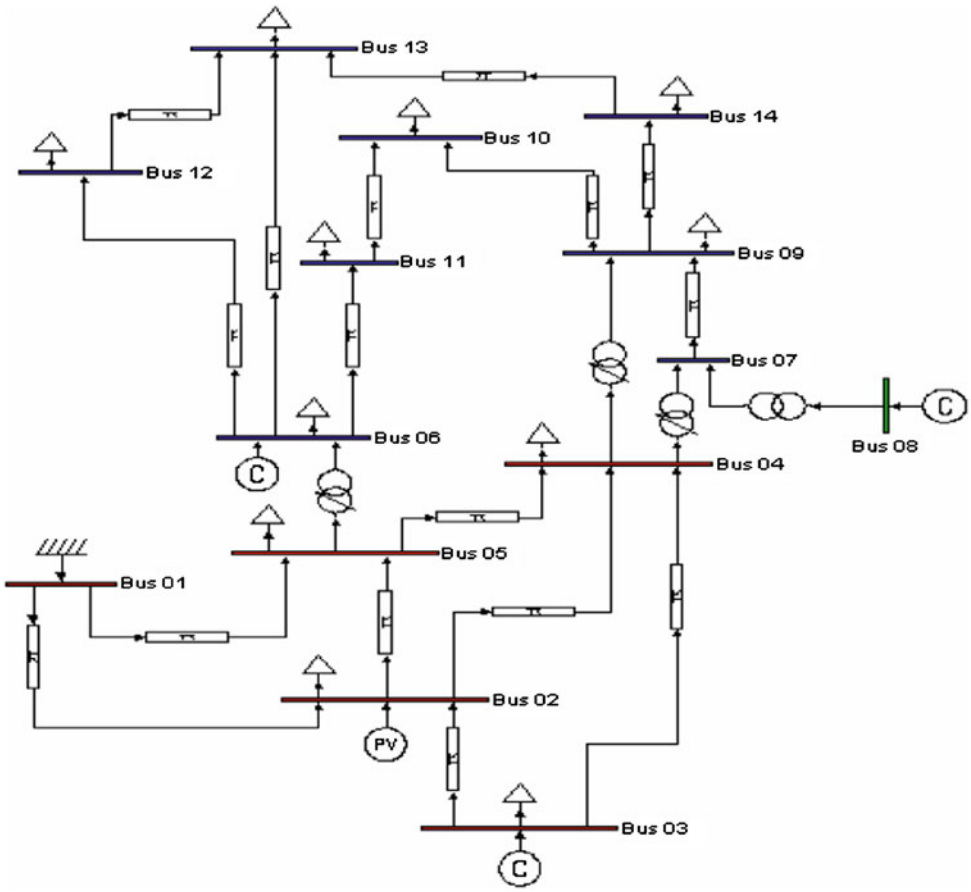

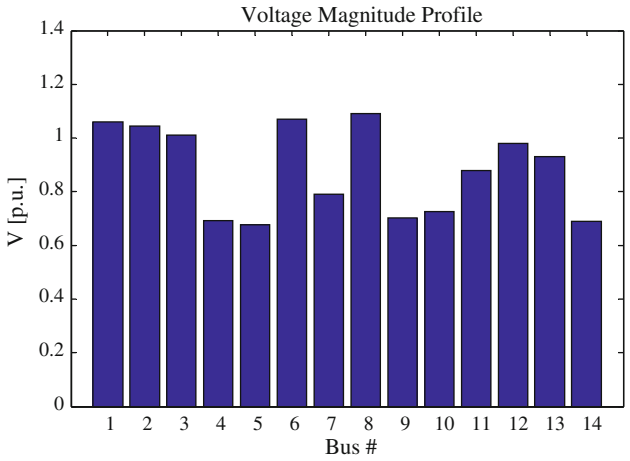

Fig. 12 Voltage magnitude profile for 14-bus test system without FACTS

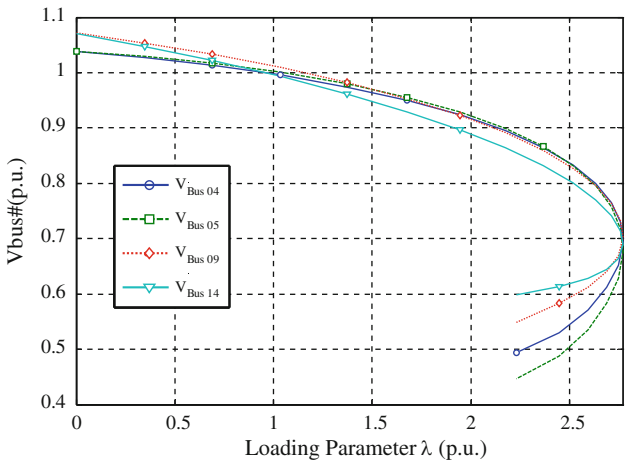

Fig. 13 PV curves for 14-bus test system without FACTS

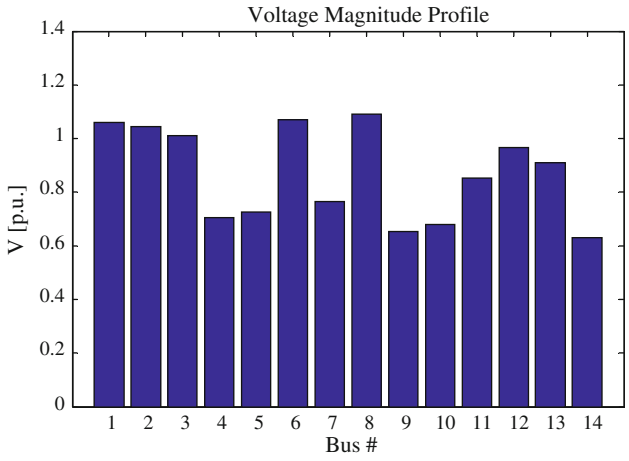

Fig. 14 Voltage magnitude profile for 14-bus test system with STATCOM

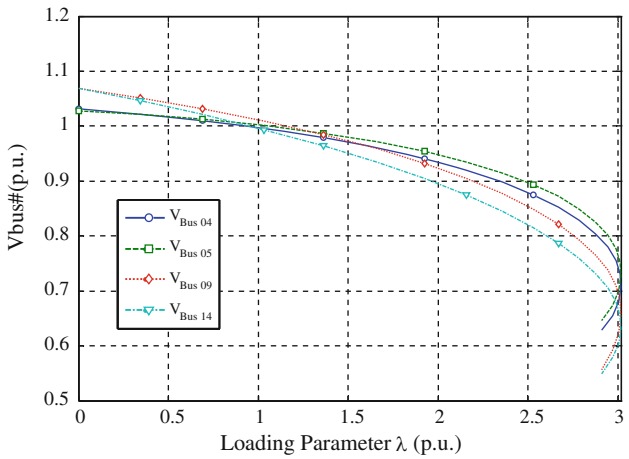

Fig. 15 PV curves for 14-bus test system with STATCOM

where P_{L0} and Q_{L0} are the active and reactive base loads, whereas P_L and Q_L, are the active and reactive loads at bus L for the current operating point as defined by λ.

From the CPF results which are shown in Fig. 12, the buses 4, 5, 9 and 14 are the critical buses. Among these buses, bus 5 has the weakest voltage profile. Voltage magnitude in MLP in bus 5 that is known as the weakest bus is 0.67636 p.u. Figure 13 shows PV curves for 14-bus test system without FACTS. The system presents a collapse or MLP, where the system Jacobian matrix becomes singular at $\lambda_{max} = 2.77$ p.u.

Based on largest entries in the right and left eigenvectors associated to the zero eigenvalue at the collapse point, bus 5 is indicated as the "critical voltage bus" needing Q support. Based on collapse analysis, bus 5 is targeted as the first location for an STATCOM. Voltage profiles at the collapse point system with STATCOM device are shown in Fig. 14. It is noticed from of Fig. 14 that bus 14 is the next weakest bus if the STATCOM is introduced at bus 5. The new maximum loading level in this condition is $\lambda_{max} = 3.0178$ p.u. (Fig. 15).

Next, remove the STATCOM, and insert the TCSC between bus 5 and bus 4, and then repeat to create PV curve again. Voltage profiles at the collapse point system with TCSC device are shown in Fig. 16.

The MLP or critical voltage point is at $\lambda_{max} = 2.7769$ p.u. (Fig. 17). TCSC is installed at line 5–4, where the reactive power is supplied only to the line, which may not improve voltage profile throughout the system. From Figs. 16 and 17, it can be observed that the improvement of voltage in these buses with STATCOM is more than the case that TCSC inserted in the system. Clearly, results show that not only the TCSC cannot increase system loadability level significantly but also may introduce a premature limit induced bifurcation.

A similar approach to the one followed to analyze the TCSC effect on maximum loadability is used to study the corresponding effects of a SSSC. Figure 18 illustrates the effects of inserting a SSSC in the candidate line.

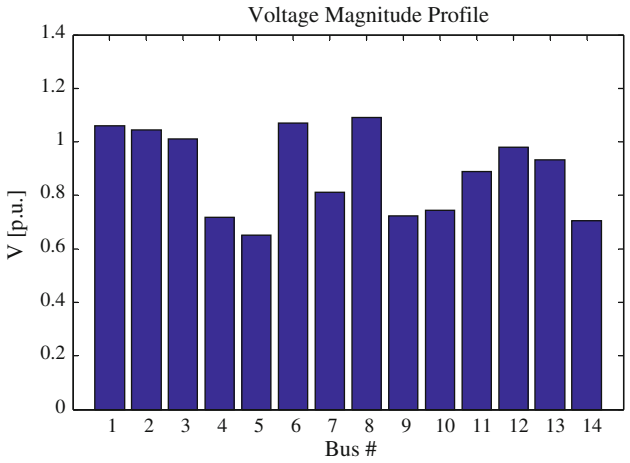

Fig. 16 Voltage magnitude profile for 14-bus test system with TCSC

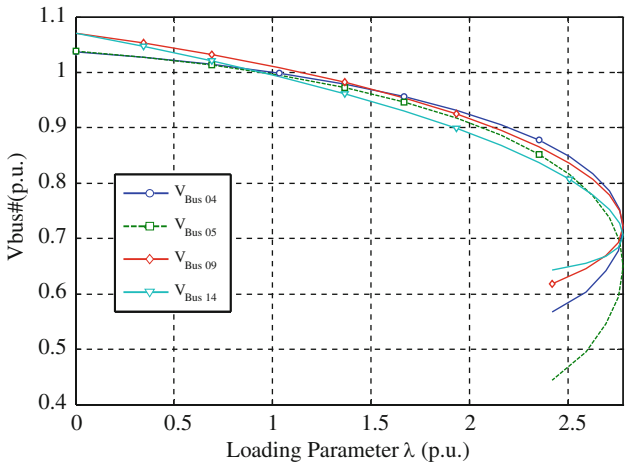

Fig. 17 PV curves for 14-bus test system with TCSC

PV curves of system with SSSC are illustrated in Fig. 19. The MLP is increasing at $\lambda_{max} = 2.791$ p.u.

Then, remove the SSSC, and insert the UPFC between bus 5 and bus 4, and then repeat to create PV curve again. Figures 20 and 21 illustrate the effects of inserting a UPFC in the candidate line. Clearly, the MLP significantly increases with respect to STATCOM, TCSC and SSSC compensation level. The new MLP in this condition is $\lambda_{max} = 3.0438$ p.u.

Figures 22 and 23 show MLP and MWM with various FACTS devices. The values of λ_{max} and MWM with all types of FACTS devices are compared in Table 1. From the table and Figs. 21 and 22, it is obvious that UPFC gives the maximum loading margin compared to other devices. Shunt compensation device injects the reactive power at the connected bus but series compensation device inserts the reactive power at the connected line.

The test system needs reactive power at the load bus more than the line. The weakest bus (bus 5) of the system is located at the load area and it requires reactive power the most.

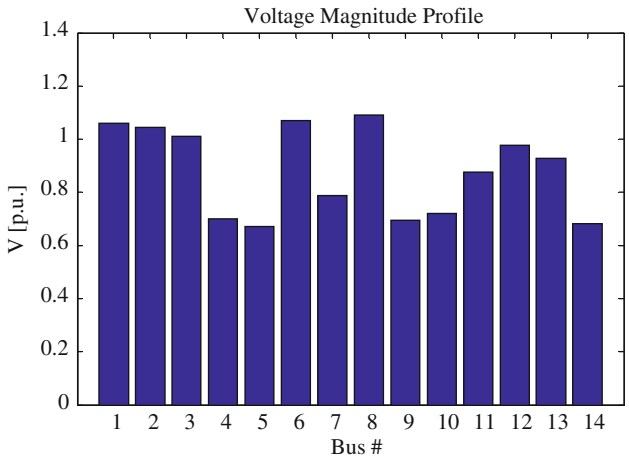

Fig. 18 Voltage magnitude profile for 14-bus test system with SSSC

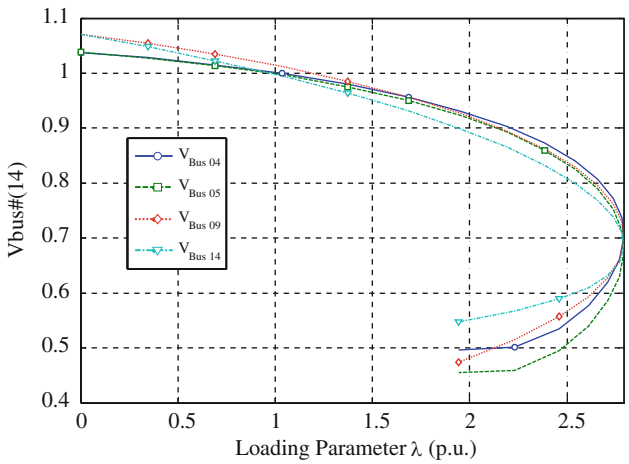

Fig. 19 PV curves for 14-bus test system with SSSC

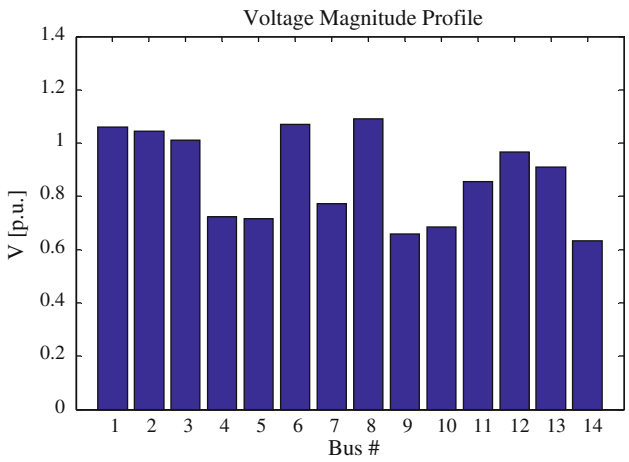

Fig. 20 Voltage magnitude profile for 14-bus test system with UPFC

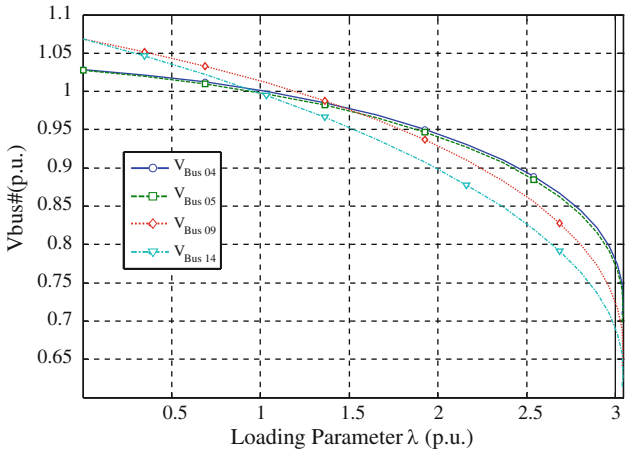

Fig. 21 PV curves for 14-bus test system with UPFC

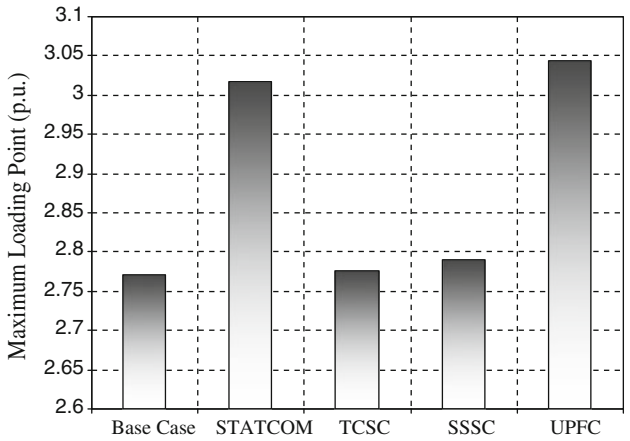

Fig. 22 MLP with various FACTS devices

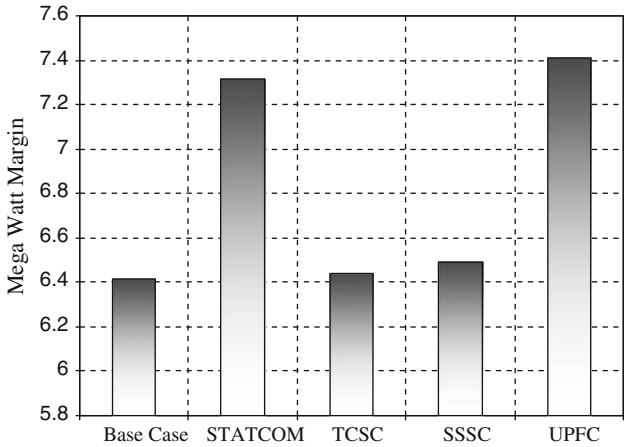

Fig. 23 MWM with various FACTS devices

6 Conclusion

In this paper, voltage stability assessment of the modified IEEE 14-bus test system with STATCOM, TCSC, SSSC and UPFC is studied. UPFC provides higher voltage stability margin than STATCOM, TCSC and SSSC. The test system requires reactive power the most at the weakest bus, which is located in the distribution level. Introducing reactive power at this bus using UPFC can improve loading margin the most. TCSC and SSSC are series compensation devices, which inject reactive power through the connected line. This may not be effective when the system required reactive power at the load level. UPFC and STATCOM give slightly higher MLP and better voltage profiles compared to TCSC and SSSC. It was found that these controllers significantly enhance the voltage profile and thus the loadability margin of power systems.

Table 1 Maximum loading point and mega Watt margin with various FACTS devices

	λ_{max} (p.u.)	P_{max} (p.u.)	P_{base} (p.u.)	MWM (p.u.)
Base case	2.77	10.0438	3.626	6.4178
STATCOM	3.0178	10.9424	3.626	7.3164
TCSC	2.7769	10.069	3.626	6.443
SSSC	2.791	10.12	3.626	6.494
UPFC	3.0438	11.0368	3.626	7.4108

References

1. Sode-Yome A, Mithulananthan N, Lee KY (2005) Static voltage stability margin enhancement using STATCOM, TCSC and SSSC. IEEE/PES transmission and distribution conference & exhibition, Asia and Pacific, Dalian, China, pp 1–6
2. Blackout of 2003. Description and responses. Available: http://www.pserc.wisc.edu/
3. Natesan R, Radman G (2004) Effects of STATCOM, SSSC and UPFC on voltage stability. In: Proceedings of the 36th southeastern symposium on system theory, pp 546–550
4. Dobson I, Chiang HD (1989) Towards a theory of voltage collapse in electric power systems. Syst Control Lett 13(3):253–262
5. Canizares CA, Alvarado FL, DeMarco CL, Dobson I, Long WF (1992) Point of collapse methods applied to ac&dc power systems. IEEE Trans Power Syst 7(2):673–683
6. Canizares CA, Faur ZT (1999) Analysis SVC and TCSC controllers in voltage collapse. IEEE Trans Power Syst 14(1):158–165
7. Sode-Yome A, Mithulananthan N (2004) Comparison of shunt capacitor, SVC and STATCOM in static voltage stability margin enhancement. Int J Electr Eng Educ (UMIST) 41(2):158–171
8. Kazemi A, Vahidinasab V, Mosallanejad A (2006) Study of STATCOM and UPFC controllers for voltage stability evaluated by Saddle-Node bifurcation analysis. In: Proceedings of the first international power and energy conference (PECon/IEEE), Putrajaya, Malaysia, pp 191–195
9. Huang GM, Zhao L, Song X (2002) A new bifurcation analysis for power system dynamic voltage stability studies. IEEE Power Eng Soc Winter Meet 2:882–887
10. Ayasun S, Nwankpa CO, Kwatny HG (2004) Computation of singular and singularity induced bifurcation points of differential– algebraic power system model. IEEE Trans Circuits Syst 51(8):1525–1538

11. Kuru L, Kuru E, Yalpm MA (2004) An application of chaos and bifurcation in nonlinear dynamical power systems. In: Proceedings of the 2nd IEEE international conference on intelligent systems, vol 3, pp 11–15
12. Perleberg Lerm A, Cafizares CA, Silva AS (2003) Multi-parameter bifurcation analysis of the South Brazilian power system. IEEE Trans Power Syst 18(2):737–746
13. Yue M, Schlueter R (2004) Bifurcation subsystem and its application in power system analysis. IEEE Trans Power Syst 19(4):1885–1893
14. Farsangi MM, Song YH, Lee KY (2004) Choice of FACTS device control inputs for damping inter-area oscillations. IEEE Trans Power Syst 19(2):1135–1143
15. Cigre 95 TP108 (1995) FACTS overview. IEEE Power Eng Soc
16. Cañizares CA (2000) Power flow and transient stability models of FACTS controllers for voltage and angle stability studies. In: Proceedings of the 2000 IEEE–PES winter meeting, vol 2. Singapore, pp 1447–1454
17. Boonpirom N, Paitoonwattanakij K (2005) Static voltage stability enhancement using FACTS. In: Proceedings of the 7th international power engineering conference IPEC/IEEE, vol 2, pp 711–715
18. Mashayekh M, Kazemi A, Jadid S (2006) A new approach for modelling of UPFC in power flow and optimum power flow studies. In: Proceedings of the 1st IEEE conference on industrial electronics and applications, pp 1–6
19. Milano F (2008) Power system analysis toolbox, version 2.1.1, software and documentation